

Supplemental Data

Contents

1 Additional materials and methods	2
1.1 General laboratory equipment	2
1.2 Cell line and animal model.....	2
1.3 Synthesis	3
1.4 Radiochemistry	3
1.4.1 Operating the $^{224}\text{Ra}/^{212}\text{Pb}$ generator	3
1.4.2 Radiolabeling.....	4
1.5 Paper electrophoresis.....	5
1.6 LogD _{7.4} values.....	5
1.7 Bismuth release in vitro	5
1.7.1 Ultrafiltration assay	5
1.7.2 C18 cartridge assay	6
1.7.3 HPLC assay.....	6
1.8 Bismuth release in cells	6
1.9 Bismuth release in vivo.....	7
1.10 Dosimetry.....	7
1.10.1 Contribution of radioactive progeny	8
1.10.2 Relative biological effectiveness	9
1.12 Pathology	9
2 Figures and Tables.....	11
Supplemental Figure 1 ^{228}Th -generator and practical considerations.....	11
Supplemental Figure 2 Chemical evaluation of the Tz compounds.....	12
Supplemental Figure 3 Purification of radiolead and the radiotracers.....	13
Supplemental Figure 4 Pharmacokinetics of ^{203}Pb -labeled Tz tracers in healthy mice.....	14
Supplemental Figure 5 Biodistribution data of ^{212}Bi]BiCl ₃	15
Supplemental Figure 6 Study designs of the <i>in vitro</i> ^{212}Bi -release.....	16
Supplemental Figure 7 Gamma-spectroscopy with ^{212}Pb and ^{208}Tl	17
Supplemental Figure 8 RBE-weighted absorbed doses estimated for ^{212}Pb]Pb-DO3A-PEG ₇ -Tz	18
Supplemental Figure 9 Biodistribution data of ^{64}Cu -labeled Tz tracers in healthy mice.....	19
Supplemental Figure 10 Hematological parameters and weights.....	20
Supplemental Figure 11 Individual tumor growth plots for all cohorts of the therapy study.....	21
Supplemental Figure 12 Re-imaging with ^{64}Cu]Cu-5B1.....	22
Supplemental Table 1 Chemical evaluation of the tetrazine compounds.....	23
Supplemental Table 2 In vitro bismuth release from the tetrazine compounds.....	23
Supplemental Table 3 RBE-weighted dose calculations assuming in situ decay of the progeny.....	24
Supplemental Table 4 RBE-weighted dose calculations considering the redistribution of the progeny.....	25
References.....	26

1 Additional materials and methods

1.1 General laboratory equipment

All instruments were calibrated and maintained in accordance with standard quality-control procedures. A Capintec CRC-55tR Dose Calibrator (Capintec, Ramsey, NJ) was used for all activity measurements except for those of harvested tissues. The activity measurements for tissues harvested in biodistribution studies were performed on a Perkin Elmer Wizard² 2480 Automatic Gamma Counter (Waltham, MA). The samples were counted for 60 sec, except for ²¹²Bi measurements, which were counted for 45 sec. Instant thin-layer chromatography (iTLC) for radio-iTLC experiments was performed on glass microfiber chromatography paper impregnated with silica gel (iTLC-SG, Agilent Technologies) with aqueous EDTA (ethylenediaminetetraacetic acid, 50 mM, pH 5.5) as the mobile phase, scanned on a Bioscan AR-2000 radioTLC plate reader, and analyzed using Winscan radio-TLC software (Bioscan Inc.). All HPLC purifications (Buffer A: 0.1% trifluoroacetic acid (TFA) in H₂O, Buffer B: 0.1% TFA in CH₃CN) were performed on a Shimadzu UFLC HPLC system equipped with a DGU-20A₃ degasser, an SPD-M20A UV detector, a LC-20AB pump system, and a CBM-20A communication BUS module, using a C18 reversed phase XTerra® Preparative MS OBD column (10 μm, 19 × 250 mm) at a constant flowrate of 8 mL/min. All analytical and radio-HPLC analyses were performed using a Shimadzu HPLC with two LC-10AT pumps, a SPD-M10AVP photodiode array detector, a Dual Scan-Ram Radio-TLC/HPLC detector (LabLogic), equipped with Universal KR-C18 column (5 μm 100 × 4.6 mm) using a gradient of 5:95 CH₃CN:H₂O (both with 0.1% TFA) to 95:5 CH₃CN:H₂O over 15 min at a constant flowrate of 1 mL/min. (Radio-) size-exclusion chromatography (SEC) was performed on the same instrument using a Yarra SEC-3000 column (3 μm 300 × 7.8 mm) and Phosphate buffered saline (PBS) as mobile phase (isocratic) at a constant flowrate of 1 mL/min. Nuclear magnetic resonance (NMR) spectroscopy was performed on a Bruker Avance III UltraShield Plus 500 MHz NMR equipped with a BBO probe. All NMR spectra were measured in Dimethyl sulfoxide-d₆ and evaluated using the MestReNova software (Version: 6.0.2-5475). Liquid chromatography–mass spectrometer (LC–MS) was performed on a C18 BEH column (100 mm with 1.7 μm particle size) using a Waters ACQUITY UPLC (Milford, MA, USA) interfaced to a single quadrupole ESI (electrospray ionization) mass spectrometer (SQD), Evaporative Light Scattering Detector (ELSD), and Photo Diode Array (PDA) Detector. High-Resolution Mass Spectrometry ("exact mass") was performed on a Waters LCT Premier XE (Milford, MA, USA). UV-Vis measurements, including antibody quantification, were taken on a Thermo Scientific NanoDrop One Spectrophotometer.

1.2 Cell line and animal model

The pancreatic cancer cell line BxPC-3 (American Type Culture Collection, ATCC) was cultured according to the recommended conditions at 5% CO₂ atmosphere and 37 °C in RPMI-1640 medium containing 10% fetal bovine serum. The MSK Media Preparation Core provided the media. For the subcutaneous xenografts, the cells were stripped in the absence of magnesium or calcium ions using a mixture of 0.25% trypsin and 0.5 mM EDTA in Hank's Balanced Salt Solution and concentrated in 1 mL of the corresponding medium. A small aliquot was used to determine the cell count (Beckman Coulter Vi-CELL XR). For the xenografts, the remaining cells were diluted with the medium so that 50 μL contained 3×10⁶ cells. All studies were performed on female athymic nude mice (CrI:NU(NCr)-Foxn1^{nu}) obtained from Charles River Laboratories (Stone Ridge, NY). After arrival, the mice () were kept in the MSK vivarium for 1 wk before any experimental handling was performed. The animals were allowed free access to water and food, and all animal care and experimental procedures were approved by the Institutional Animal Care and Use Committee (IACUC). Before the treatment, the mice were on a Sulfatrim diet to prevent skin infections. For the subcutaneous xenografts, a 1:1 ratio of Corning Matrigel Matrix and the cell solution was prepared and stored on ice for the injections. Each mouse received a subcutaneous injection of 100 μL (50 μL cell solution, 3×10⁶ cells, viability > 95%, + 50 μL Matrigel) into the flank on the level of the right shoulder. The injections were performed under anesthesia (2% isoflurane, Baxter Healthcare, Deerfield, IL, USA). Palpable tumors of similar size (100–200 mm³) developed 4–5 wk after grafting. The radiotracer administration was performed via tail vein injection.

1.3 Synthesis

The 5B1-TCO antibody conjugate (approximately three TCO moieties per mAb) was synthesized as previously published (1). The final tetrazine (Tz) conjugates were assembled by reacting the functionalized tetrazine Tz-PEG₇-NH₂ with a bifunctional version of the corresponding chelator, as previously published (2). *p*-SCN-Bn-DOTA, DOTA-NHS-ester, and *p*-SCN-Bn-TCMC were purchased from Macrocyclics. *p*-SCN-Bn-PSC was provided by Perspective Therapeutics, Inc. All other chemicals were purchased from Sigma-Aldrich and used as received. The identity and purity of the synthesized compounds were confirmed via ¹H- and ¹³C-NMR (nuclear magnetic resonance) and ESI MS (electrospray ionization mass spectrometry). The analysis for DOTA-PEG₇-Tz did match the literature records (2).

Analytical data for PSC-PEG₇-Tz were as follows: bright pink solid; ¹H NMR (500 MHz, DMSO-d₆) ppm: δ = 12.81 (s, 1H), 10.58 (s, 1H), 9.69 (s, 1H), 8.98 (s, 1H), 8.47 (m, 2H), 7.98 (s, 1H), 7.87 (t, 1H), 7.79 (t, 1H), 7.72 (s, 1H), 7.54 (d, 2H), 7.42 (d, 2H), 7.25 (d, 2H), 4.39 (d, *J* = 5.9 Hz, 2H), 4.33 (d, *J* = 5.3 Hz, 2H), 4.09 (s, 2H), 3.99 (s, 4H), 3.55 (m, 11H), 3.50 (m, *J* = 6.5 Hz, 24H), 3.40 (t, 4H), 3.19 (q, *J* = 11.6, 5.8 Hz, 2H), 3.07 (bs, 8H), 2.18 (t, *J* = 7.5 Hz, 2H), 2.10 (t, *J* = 14.9, 7.4 Hz, 2H), 1.76 (q, 2H) ¹³C NMR (126 MHz, DMSO-d₆) δ 180.76, 172.33, 172.01, 171.81, 165.43, 158.13, 157.85, 157.61, 145.06, 130.33, 128.07, 127.82, 125.92, 122.99, 117.83, 115.38, 69.75, 69.59, 69.14, 68.56, 54.84, 52.27, 51.08, 47.49, 43.54, 41.83, 38.46, 34.73, 21.51; HRMS (ESI) — *m/z* calculated for C₅₄H₈₄N₁₄O₁₅S: 1200.60 u; found: [M+H]⁺ 1201.64.

Analytical data for DO3A-PEG₇-Tz were as follows: bright pink solid; ¹H NMR (500 MHz, DMSO-d₆) ppm: δ = 13.03 (s, 1H), 10.58 (s, 1H), 8.58 (s, 1H), 8.46 (d, *J* = 8.1 Hz, 2H), 7.88 (t, *J* = 5.4 Hz, 1H), 7.53 (d, *J* = 8.2 Hz, 2H), 4.39 (d, *J* = 5.8 Hz, 3H), 3.50 (m, 25H), 3.40 (m, 11H), 3.28 (d, *J* = 5.5 Hz, 4H), 3.19 (q, 2H), 3.11 (s, 8H), 2.54 (s, 5H), 2.18 (t, 2H), 2.10 (t, 2H), 1.77 (q, 2H) ¹³C NMR (126 MHz, DMSO-d₆) δ 172.02, 171.83, 165.43, 158.43, 145.06, 130.35, 128.07, 127.82, 117.41, 115.07, 69.77, 69.57, 69.14, 68.73, 52.48, 50.48, 45.75, 41.79, 40.43, 38.46, 34.73, 21.51; HRMS (ESI) — *m/z* calculated for C₄₆H₇₅N₁₁O₁₆: 1037.54 u; found: [M+H]⁺ 1038.60.

Analytical data for TCMC-PEG₇-Tz were as follows: bright pink solid; ¹H NMR (500 MHz, DMSO-d₆) p.p.m.: δ = 10.6 (s, 1H), 9.69 (s, 1H), 8.47 (d, *J* = 8.3 Hz, 2H), 7.88 (s, 1H), 7.82 (m, 1H), 7.74 (m, 1H), 7.62 (m, 1H), 7.54 (s, *J* = 8.2 Hz, 1H), 7.47 (d, *J* = 8.2 Hz, 2H), 7.23 (d, *J* = 10.3 Hz, 2H), 7.12 (s, 1H), 7.02 (s, 1H), 4.40 (d, *J* = 5.9 Hz, 2H), 3.51 (m, 18H), 3.40 (m, *J* = 6.3 Hz, 36H), 3.20 (m, 2H), 3.10 (m, *J* = 7.3 Hz, 2H), 2.19 (m, 2H), 2.11 (m, *J* = 7.6 Hz, 2H), 1.77 (m, 2H), 1.18 (t, *J* = 7.3 Hz, 2H); HRMS (ESI) — *m/z* calculated for C₅₄H₈₆N₁₆O₁₃S: 1198.63 u; found: [M+H]⁺ 1199.71.

1.4 Radiochemistry

! INFORMATION All chemicals used were of high purity. Trace metal-free water was purchased from Honeywell Riedel-de Haën (TraceSELECT) and hydrochloric acid from Fisher Chemical (TraceMetal Grade). Other solvents and buffers were purified over Chelex 100 Resin (200–400 mesh, sodium form, BIO-RAD) to minimize the trace metal content.

The ²²⁴Ra/²¹²Pb generators were received either from Perspective Therapeutics, Inc. or the US Department of Energy Isotope Program (370 MBq).

[²⁰³Pb]PbCl₂ was either received from the Medical Isotope and Cyclotron Facility of the University of Alberta (Edmonton, Canada) or the Cyclotron Facility of the University of Alabama at Birmingham (USA). If necessary, ²⁰³Pb was purified by the same method described below for ²¹²Pb.

[⁶⁴Cu]CuCl₂ was received from 3D Imaging LLC (Little Rock, AR) as a 0.1 M HCl solution.

1.4.1 Operating the ²²⁴Ra/²¹²Pb generator

! CAUTION ²²⁴Ra decays through the alpha-emitting noble gas ²²⁰Rn (*t*_{1/2} = 55.6 sec). The generators should be operated in a well-ventilated chemical hood, and the column should be loaded with water.

! INFORMATION The ²²⁴Ra/²¹²Pb generator can be eluted in a 24 h interval to obtain 75% ²¹²Pb (compared to available ²²⁴Ra activity). The maximum of available ²¹²Pb can be eluted in 1.4 d intervals. ²¹²Bi can be eluted in 3 h intervals.

The $^{224}\text{Ra}/^{212}\text{Pb}$ generator consists of a Teflon column loaded with ^{224}Ra -containing resin (AG MP50, 100–200 mesh) embedded in a lead cylinder. After receiving the generators (shipped with dry column), they were stored in water to decrease the ^{220}Rn release and increase the ^{212}Pb yield. During the use period of 2 wk, no release of ^{220}Rn was detected. After each elution, 1 mL of water was loaded onto the column for overnight storage.

! INFORMATION When measuring the ^{212}Pb activity via a dose calibrator, the value can be easiest obtained when measuring freshly purified ^{212}Pb (daughter free) of ^{212}Pb in equilibrium (8 h after purification). Alternatively, individual multiplication factors for each time point have to be applied. In this work, the initial activities were measured on a CRC–55tR Dose Calibrator with the 101 Calibration Setting Number for purified ^{212}Pb . After the initial measurement, activities were calculated by volume.

Before the elution, the storage water was removed by flushing the generator with air. Next, ^{212}Bi was removed by washing the generator with 1 mL of 0.5 M HCl solution, followed by rinsing the generator with air. Finally, ^{212}Pb was eluted with 2 mL of 2 M HCl solution, and the generator was loaded with water for overnight storage.

The lead was additionally purified over Pb Resin (20–50 μm , Eichrom Technologies). Briefly, 40–60 mg of resin was suspended in 0.5 mL of 2 M HCl solution and packed on a 1 mL pre-fitted polypropylene cartridge (Supelco, 54220–U, Sigma–Aldrich). The cartridge was equilibrated with 2 mL of 0.5 M HCl solution and flushed with air. The ^{212}Pb solution (2 mL in 2 M HCl) was diluted with 6 mL of water to obtain a final HCl concentration of 0.5 M. This solution was loaded onto the cartridge at a rate of 1 mL/min. At this pH, the Pb Resin retains Pb^{2+} ions.

Further impurities and daughter nuclides were removed by washing the cartridge with 1 mL of 0.5 M HCl solution. Finally, the purified and daughter-free ^{212}Pb was eluted with 2 mL NH_4OAc solution (1 M, pH 4.5), and the activity was measured immediately. The elution profile can be found in Supplemental Figure 3A.

For only eluting ^{212}Bi , first, the storage water was removed by flushing the generator with air. Next, ^{212}Bi was eluted by slowly flushing the generator with 1 mL of 0.5 M HCl solution, then rinsing it with air and storing it in water. The ^{212}Bi solution was purified by passing it through a Pb Resin cartridge (as described above) at a 1 mL/min rate to remove lead impurities. The ^{212}Bi was obtained in the eluate.

1.4.2 Radiolabeling

! INFORMATION All tetrazine precursors were dissolved in DMSO (dimethyl sulfoxide) to obtain a stock solution with a concentration of 10^{-3} M (1 μL stock solution = 1 nmol precursor). For animal studies, each mouse received 1–2 nmol of radiolabeled tetrazine.

! INFORMATION Under the abovementioned conditions, the chelators do not chelate ^{212}Bi or other daughter nuclides. The radio iTLC for ^{212}Pb -labeled precursors will show free daughter nuclides and can be reevaluated after the equilibrium is reached (8 h) to be quantitatively analyzed. A complete ^{212}Pb and ^{212}Bi -labeling can be achieved by heating up the reaction mixture to 95 $^{\circ}\text{C}$ for 5 min.

For radiolabeling with purified $^{203/212}\text{Pb}$ obtained in 2 mL of NH_4OAc buffer (1 M, pH 4.5), the required amount (e.g., 100–1000 μL) was aliquoted into a 2 mL microcentrifuge tube, and the required amount of tetrazine stock solution (e.g., 5–50 μL) was added. Radiolabeling was found to be reliably quantitative at a chelator concentration of 10^{-4} M to 5×10^{-6} M. The mixture was reacted for 10 min at room temperature, and radiolabeling was confirmed via radio iTLC.

After confirmed radiolabeling, the radiotracer was loaded on a C18 cartridge (Strata-X 33 μm Polymeric Reversed Phase, 30 mg/1 mL tubes), washed with PBS (1 mL), and eluted with ethanol (200 proof, 95%) to obtain the purified and daughter free radiotracer. For ^{212}Pb -labeled precursors, the activity was measured immediately after elution (setting for purified lead). After the initial measurement, activities were calculated by volume. A typical elution profile can be found in Supplemental Figure 3 B.

For radiolabeling with $^{64}\text{Cu}[\text{CuCl}_2]$ or $^{203}\text{Pb}[\text{PbCl}_2]$, received as a hydrochloric acid solution, the required activity was transferred to a 2 mL microcentrifuge tube, and the 20-fold amount of NH_4OAc buffer (1 M, pH 4.5) was added together with the corresponding tetrazine precursor, the mixture was reacted for 20 min at room temperature. Radiolabeling was reliably quantitative at a chelator concentration of 10^{-4} M to 5×10^{-6} M. Radiolabeling was confirmed via radio iTLC. All radiotracers were purified via a C18 cartridge, as described above.

1.5 Paper electrophoresis

This procedure was adapted from the literature (3). Paper electrophoresis was performed on 1 × 20 cm cellulose chromatography paper stripes (3001-861, Grade 1 Chr, Whatman) using an Owl EasyCast B2 electrophoresis system (Thermo Scientific) with a Bio-Rad 1000/500 constant voltage power supply. The running buffer consisted of 1 × PBS with 0.1 M 4-(2-hydroxyethyl)-1-piperazineethanesulfonic acid (HEPES), pH-adjusted to 7.4. Directly before the run, the radiotracer (3.7–185 kBq) was placed in the middle of a pre-wetted paper strip. Paper electrophoresis was run at 180 volts for 2 h. Up to 6 strips were placed at the same time. Each tracer was run in triplicates. Before the evaluation, the paper stripes were dried, sealed in Parafilm, and exposed to a phosphor-imaging plate (Fujifilm BAS-MS2325, Fuji Photo Film, Japan) in a film cassette. The film was read using a Typhoon 8600 photographic film scanner (GE Healthcare). The data were analyzed and plotted with ImageJ2 freeware (Fiji).

1.6 LogD_{7.4} values

This procedure was adapted from the literature (4). Briefly, 450 µL 1-octanol and 448 µL PBS were added to a 2 mL microcentrifuge tube, and the two phases were equilibrated for 1 h. Following, 2 µL of the radiotracer (37–370 kBq) was added, and the phases were mixed at room temperature for 2 h in a rotating mixer. The phases were separated by centrifugation (4000 rpm, 2 min), and 10 µL of the aqueous phase and 200 µL of the organic phase were aliquoted into a conical tube for gamma counting and measured for 4 min each. The logD_{7.4} value was calculated as follows:

$$\log D_{7.4} = \log_{10} \left(\frac{\text{cpm in } 200 \mu\text{L octanol}}{\text{cpm in } 10 \mu\text{L PBS} \times 20} \right) \quad \text{Eqn. S1}$$

The tracers were evaluated in quadruplicates. The results are displayed in Supplemental Table 1.

1.7 Bismuth release in vitro

Upon the first decay, the ²¹²Pb-labeled radiotracers partially retain the first daughter nuclide ²¹²Bi. Various methods were employed to determine and verify the percentage of ²¹²Bi release from the chelators.

! INFORMATION These methods are based on relative activity ratios and do not require the exact measurements of the total activity.

! INFORMATION ²¹²Bi is a relatively low-yield gamma emitter. The released bismuth was determined via the next daughter nuclide ²⁰⁸Tl (t_{1/2} = 3.1 min; 583 keV, 85%). An adequate equilibrium is reached after 15 min. The gamma counter was set up for a specific window of (583 ± 50) keV (Supplemental Figure 7).

! INFORMATION The final chelator concentration in all ²¹²Bi release experiments ranged between 10⁻⁷ to 10⁻⁸ M. Under these concentrations, no (re-)chelation of ²¹²Pb (or ²¹²Bi) was observed.

! INFORMATION The influence of radiolysis was negligible at the activity concentrations used. Radiolysis would lead to a release of ²¹²Pb from the radiotracers. For all ²⁰⁸Tl measurements at the gamma counter, an additional window of (239 ± 50) keV for ²¹²Pb was added. ²¹²Pb-release was measured to be less than 2% in all experiments.

! INFORMATION The ultrafiltration and the C18 cartridge assay involved elution steps with aqueous EDTA solution (50 mM, pH 7). This solution was also investigated as a running buffer in the radio iTLCs. Under these conditions, no transchelation of ²¹²Pb- of ²¹²Bi-labeled was observed for the mentioned chelators.

1.7.1 Ultrafiltration assay

First, the four radiotracers (10 nmol of DOTA-PEG₇-Tz, DO3A-PEG₇-Tz, PSC-PEG₇-Tz, and TCMC-PEG₇-Tz) were radiolabeled with ²¹²Pb (3.7 MBq each) and purified as described above. The tetrazine-bearing radiotracer was separately clicked to 100 µg of 5B1-TCO. Alternatively, the experiment was repeated with 100 µg of a TCO-conjugated IgG4 control antibody. The radio-conjugates were transferred into centrifugal filters (Amicon™ Ultra-0.5 mL Centrifugal Filter Units, 30 kD molecular weight cutoff, pre-washed with PBS) and purified via ultrafiltration by three wash steps (2 × 400 µL 50 mM EDTA at pH 7, 1 × 400 µL PBS).

For each purified radio-conjugate, the sample was split into four aliquots of approx. 0.2 MBq and transferred into four new centrifugal filters and topped off with PBS. The aliquots were stored overnight (at least 8 h) at room temperature to reach the equilibrium between mother and daughter nuclide. Next, the centrifugal

filters were spun down and washed using an EDTA solution (2 x 200 µL, 50 mM at pH 7). The filters (chelated ²¹²Bi) and filtrates (released ²¹²Bi) were measured individually for each aliquot in the gamma counter precisely 15 min after starting the separation process (*cpm_{initial}*). After the equilibrium was reached, the samples were remeasured the next day, and the cpm (counts per min) were back calculated to the initial measurement time (*cpm_{rem-bc}*).

The daughter nuclide release was calculated either via:

$${}^{212}\text{Bi release} = \frac{\textit{cpm}_{\textit{initial}} \textit{ (released)}}{\textit{cpm}_{\textit{initial}} \textit{ (released)} + \textit{cpm}_{\textit{initial}} \textit{ (chelated)}} \times 100\% \quad \text{Eqn. S2}$$

or

$${}^{212}\text{Bi release} = \frac{\textit{cpm}_{\textit{rem-bc}} \textit{ (chelated)} - \textit{cpm}_{\textit{initial}} \textit{ (chelated)}}{\textit{cpm}_{\textit{rem-bc}} \textit{ (chelated)}} \times 100\% \quad \text{Eqn. S3}$$

It was found that calculations via Eqn. S3 lead to a smaller distribution of errors. However, both methods lead to comparable values. The random error was found to be smaller than 2% for all measurements. The systematic error was anticipated to be around 5% which was used as the one-sigma standard deviation. This assay is illustrated in Figure 6C.

1.7.2 C18 cartridge assay

This procedure was adapted from the literature (5). After radiolabeling and purification, the radiotracer (approx. 5 µL, 0.2 MBq) was diluted with 500 µL PBS. The solution was loaded onto a C18 cartridge (Strata-X 33 µm Polymeric Reversed Phase, 30 mg/1 mL tubes) but not passed through. The aliquots were stored overnight (at least 8 h) at room temperature to reach the equilibrium between mother and daughter nuclide. Next, the cartridge was eluted into an Eppendorf and washed using an EDTA solution (2 x 500 µL, 50 mM at pH 7). The cartridge and the combined eluted fractions were measured precisely 15 min after starting the separation process, and the release was calculated as described above for the ultrafiltration assay. Each radiotracer was evaluated in quadruplicates. This assay is illustrated in Figure 6A.

1.7.3 HPLC assay

After radiolabeling and purification, the radiotracer (approx. 5 nmol, 0.2 MBq) was diluted with 100 µL PBS and equilibrated overnight (but at least 8 h). An aliquot of 90 µL was injected into the HPLC (Universal KR-C18 column (5 µm 100 x 4.6 mm), using a gradient of 5:95 CH₃CN:H₂O (both with 0.1% TFA) to 95:5 CH₃CN:H₂O over 15 min at a constant flowrate of 1 mL/min). The injection peak (released ²¹²Bi) was found to elute at 3 min post-injection, and the radiotracers (chelated ²¹²Bi) eluted between minutes 8 and 9. Since ²¹²Bi does not show a detectable gamma signature, the first fraction (released ²¹²Bi) was collected from minute 2–6, and the second fraction (chelated ²¹²Bi) from minute 7–11. The bismuth release was calculated most reproducibly by employing Eqn. S3 and only using the second fraction, initially measured 15 min after starting the collection and remeasured the next day. More details can be found above in the ultrafiltration assay section. The experiment was run in triplicates. This assay is illustrated in Figure 6B.

1.8 Bismuth release in cells

Before starting this assay, four 6-well cell culture plates (FB012927, Fisherbrand) were seeded with 0.5 x 10⁶ BxPC-3 cells per well and incubated for two days. The media was exchanged daily. On the third day, the wells were 80% confluent.

As described in the ultrafiltration assay section, the radiotracer of choice was clicked to 5B1-TCO, and the conjugate was purified. Next, the ²¹²Pb-labeled antibody was mixed with cold cell media and added to two 6-well cell culture plates (approx. 37 kBq, and 1 µg antibody per well). The plates were incubated at 4 °C for 3 h, followed by washing steps (3 x 1 mL PBS) to remove excess unbound antibodies. After 1 mL of cold media was added to each well, one plate was incubated overnight for 9 h at 4 °C, and the second at 37 °C. Following, all plates were stored at 4 °C for 5 h before being processed.

The remaining two 6-well cell culture plates were incubated with free ²¹²Bi (74 kBq per well mixed with media) and incubated for 1.5 h at 4 °C, and at 37 °C, respectively.

After the incubation period, the media (released ^{212}Bi) was collected in gamma counter tubes with 2 wash fractions (1 mL 50 mM EDTA at pH 7) for each well. The cells (retained ^{212}Bi) were collected in a separate tube by digesting them with 1 M NaOH solution (2 × 1 mL). For each well, the two fractions were measured on the gamma counter 15 min after starting the separation and remeasured the next day. The calculation for the ^{212}Bi release ($n = 3$) can be found above. This assay is illustrated in Supplemental Figure 6D.

1.9 Bismuth release in vivo

To study ^{212}Bi distribution in vivo, four healthy mice were injected with purified and neutralized $[\text{}^{212}\text{Bi}]\text{BiCl}_3$ (1.9 MBq in 150 μL PBS), prepared as described above. The mice were euthanized 1 h post-injection, and tissue samples of interest were collected and immediately measured on the gamma counter.

To study the ^{212}Bi release in vivo, four tumor-bearing mice received pretargeting using the radiotracer $[\text{}^{212}\text{Pb}]\text{Pb-DO3A-PEG}_7\text{-Tz}$ (2 nmol, 3.7 MBq). The mice were euthanized individually 24 h post-injection, tissues of interest were collected, and samples were measured on the gamma counter on a setting specific for ^{212}Bi (more accurate ^{208}Tl (583 ± 50) keV) precisely 15 min after the time of death. All samples were remeasured the next day after they reached equilibrium with ^{212}Pb . The counts of the remeasured samples were backcalculated to the timepoint of the first measurement. The bismuth release was calculated by employing Eqn. S2 (SI). Tissue samples with positive values (e.g., tumors) indicate a net source of *in vivo* ^{212}Bi release, and tissue samples with a negative value (e.g., liver) indicate an *in vivo* ^{212}Bi sink.

1.10 Dosimetry

Using the assumption that the %ID/g is equivalent between $[\text{}^{212}\text{Pb}]\text{Pb-DO3A-PEG}_7\text{-Tz}$ and $[\text{}^{203}\text{Pb}]\text{Pb-DO3A-PEG}_7\text{-Tz}$, dosimetry estimates for murine administration of $[\text{}^{212}\text{Pb}]\text{Pb-DO3A-PEG}_7\text{-Tz}$ (3–4 days post-administration of 100 μg of 5B1-TCO conjugate) were obtained using the MOBY (6) computational mouse phantom in PARaDIM software (7). The MIRd notation is adopted here for description of the dosimetric quantities and methods (8). ^{212}Pb activity-time curves for each source region (e.g., organ, tumor, or other tissue) of the MOBY phantom, denoted r_s^{phantom} , were extrapolated from the $[\text{}^{203}\text{Pb}]\text{Pb-DO3A-PEG}_7\text{-Tz}$ murine biodistribution measurements using the following equation:

$$a(r_s, t, {}^{212}\text{Pb}) = \overline{[\%ID/g]}(r_s^{\text{mouse}}, t, {}^{203}\text{Pb}) \cdot \frac{M(r_s^{\text{phantom}})}{100\%} \cdot e^{-\lambda_p t} \quad \text{Eqn. S4}$$

where $a(r_s, t)$ is the extrapolated non-decay corrected fraction of administered activity in phantom source region r_s , $M(r_s^{\text{phantom}})$ is the mass of phantom source region r_s in units of grams, and λ_p is the physical decay constant for ^{212}Pb . $\overline{[\%ID/g]}(r_s^{\text{mouse}}, t, {}^{212}\text{Pb})$ is the percentage of administered activity of ^{212}Pb per gram of the corresponding harvested mouse tissue, averaged over the replicate mouse measurements at each time point. Equation S4 implicitly assumes the total body mass and fractional organ masses of the mice are consistent with those of the phantom; therefore, the phantom was scaled to the mean body mass of the mouse cohort (~25 g) using the phantom mass scaling function within PARaDIM. Finally, as a conservative assumption, it is assumed that the uptake in the blood is representative of the uptake in the hematopoietic bone marrow.

The fraction of administered activity in each source region was then fit by non-linear least squares regression using the Microsoft Excel Solver add-in. The fit function used was an exponential of the form:

$$a(r_s, t, {}^{212}\text{Pb}) = C_1 e^{-(\lambda_{b1} + \lambda_p)t} + C_2 e^{-(\lambda_{b2} + \lambda_p)t} \quad \text{Eqn. S5}$$

where parameters λ_{b1} and λ_{b2} are biological clearance rate constants for different phases of clearance, and C_1 and C_2 are the corresponding amplitude coefficients. To compute the total number of nuclear transformations per unit activity administered within each source region, $\tilde{a}(r_s)$ – i.e., the time-integrated

activity coefficient (TIAC) or residence time – the optimized parameters were input into the analytic expression for the time-integral of Eqn. S5, namely:

$$\tilde{a}(r_s, {}^{212}_{82}\text{Pb}) = \int_0^{\infty} C_1 e^{-(\lambda_{b1} + \lambda_p)t} + C_2 e^{-(\lambda_{b2} + \lambda_p)t} dt = \frac{C_1}{\lambda_{b1} + \lambda_p} + \frac{C_2}{\lambda_{b2} + \lambda_p} \quad \text{Eqn. S6}$$

The clearance parameters for the whole body were used to determine the TIAC for the urinary bladder contents using a dynamic voiding bladder excretory model; (9) a 1.3 h voiding interval was assumed.

1.10.1 Contribution of radioactive progeny

Regarding the fate of the radioactive progeny of ${}^{212}\text{Pb}$, two cases were considered.

Case 1: No redistribution

In the first case, it is assumed that no redistribution of progeny occurs (i.e., all progeny decay at the same site as the parent ${}^{212}\text{Pb}$). In this case, the TIACs for the source regions were computed as follows:

$$\tilde{a}(r_s, {}^{212}_{83}\text{Bi}) = B_{{}^{212}_{82}\text{Pb} \rightarrow {}^{212}_{83}\text{Bi}} \tilde{a}(r_s, {}^{212}_{82}\text{Pb}) \quad \text{Eqn. S7}$$

$$\tilde{a}(r_s, {}^{212}_{84}\text{Po}) = B_{{}^{212}_{83}\text{Bi} \rightarrow {}^{212}_{84}\text{Po}} \tilde{a}(r_s, {}^{212}_{83}\text{Bi}) \quad \text{Eqn. S8}$$

$$\tilde{a}(r_s, {}^{208}_{81}\text{Tl}) = B_{{}^{212}_{83}\text{Bi} \rightarrow {}^{208}_{81}\text{Tl}} \tilde{a}(r_s, {}^{212}_{83}\text{Bi}) \quad \text{Eqn. S9}$$

where the decay branching ratios are given by $B_{{}^{212}_{82}\text{Pb} \rightarrow {}^{212}_{83}\text{Bi}} = 1.00$, $B_{{}^{212}_{83}\text{Bi} \rightarrow {}^{212}_{84}\text{Po}} = 0.641$, and $B_{{}^{212}_{83}\text{Bi} \rightarrow {}^{208}_{81}\text{Tl}} = 0.359$.

The data is summarized in Supplemental Table 3.

Case 2: Redistribution

For the second case, we note that previous investigations of the biodistribution of free ionic bismuth have shown or suggested rapid uptake and marked retention in the kidneys. Considering the half-life of ${}^{212}\text{Bi}$ is relatively long in comparison to the timescale for kidney accumulation, it was conservatively assumed that within tissue regions, ${}^{212}\text{Bi}$ released from the chelate is immediately reabsorbed by circulating blood and instantaneously translocated to the kidneys, where it decays without excretion. For the contents of the gastrointestinal tract and urinary bladder regions (denoted 'content' regions in the proceeding equations), no reabsorption was assumed. The fraction of ${}^{212}\text{Bi}$ released from the chelator, f_R , was estimated from in vitro studies. Progeny of ${}^{212}\text{Bi}$ is short-lived and was assumed to decay at the sites of ${}^{212}\text{Bi}$ decay. The TIACs for the ${}^{212}\text{Pb}$ progeny in the kidneys are given by:

$$\tilde{a}(\text{kidneys}, {}^{212}_{83}\text{Bi}) = B_{{}^{212}\text{Pb} \rightarrow {}^{212}_{83}\text{Bi}} (1 - f_R) \tilde{a}(\text{kidneys}, {}^{212}_{82}\text{Pb}) + B_{{}^{212}\text{Pb} \rightarrow {}^{212}_{83}\text{Bi}} f_R \sum_{r_s \neq \text{content}} \tilde{a}(r_s, {}^{212}_{82}\text{Pb}) \quad \text{Eqn. S10}$$

$$\tilde{a}(\text{kidneys}, {}^{212}_{84}\text{Po}) = B_{{}^{212}_{83}\text{Bi} \rightarrow {}^{212}_{84}\text{Po}} \tilde{a}(\text{kidneys}, {}^{212}_{83}\text{Bi}) \quad \text{Eqn. S11}$$

$$\tilde{a}(\text{kidneys}, {}^{208}_{81}\text{Tl}) = B_{{}^{212}_{83}\text{Bi} \rightarrow {}^{208}_{81}\text{Tl}} \tilde{a}(\text{kidneys}, {}^{212}_{83}\text{Bi}) \quad \text{Eqn. S12}$$

The TIACs for the ${}^{212}\text{Pb}$ progeny in the urinary bladder and gastrointestinal tract contents regions are given by:

$$\tilde{a}(\text{content}, {}^{212}_{83}\text{Bi}) = B_{{}^{212}\text{Pb} \rightarrow {}^{212}_{83}\text{Bi}} \tilde{a}(\text{content}, {}^{212}_{82}\text{Pb}) \quad \text{Eqn. S13}$$

$$\tilde{a}(\text{content}, {}^{212}_{84}\text{Po}) = B_{212_{83}\text{Bi} \rightarrow 212_{84}\text{Po}} \tilde{a}(\text{content}, {}^{212}_{83}\text{Bi}) \quad \text{Eqn. S14}$$

$$\tilde{a}(\text{content}, {}^{208}_{81}\text{Tl}) = B_{212_{83}\text{Bi} \rightarrow 208_{81}\text{Tl}} \tilde{a}(\text{content}, {}^{212}_{83}\text{Bi}) \quad \text{Eqn. S15}$$

and, the TIACs for the remaining regions are given by:

$$\tilde{a}(r_S \neq \text{kidneys}, \text{content}, {}^{212}_{83}\text{Bi}) = B_{212_{82}\text{Pb} \rightarrow 212_{83}\text{Bi}} (1 - f_R) \tilde{a}(r_S, {}^{212}_{82}\text{Pb}) \quad \text{Eqn. S16}$$

$$\tilde{a}(r_S \neq \text{kidneys}, \text{content}, {}^{212}_{84}\text{Po}) = B_{212_{83}\text{Bi} \rightarrow 212_{84}\text{Po}} \tilde{a}(r_S, {}^{212}_{83}\text{Bi}) \quad \text{Eqn. S17}$$

$$\tilde{a}(r_S \neq \text{kidneys}, \text{content}, {}^{208}_{81}\text{Tl}) = B_{212_{83}\text{Bi} \rightarrow 208_{81}\text{Tl}} \tilde{a}(r_S, {}^{212}_{83}\text{Bi}) \quad \text{Eqn. S18}$$

The data is summarized in Supplemental Table 4.

1.10.2 Relative biological effectiveness

The contributions to the absorbed dose coefficient from each chain member were computed by Monte Carlo simulation in PARaDIM, using the TIACs computed above. Relative biological effectiveness-weighted (RBE-weighted) dose coefficients were obtained by multiplying the absorbed dose contributions of alpha particles by a factor of 5, reflecting the relative biological effectiveness of alpha particles toward deterministic endpoints (e.g., therapy, toxicity). For beta particles and photons, RBE-weighting factors of 1 were used. Finally, the contributions were summed to obtain the RBE-weighted dose coefficient for each target organ.

1.12 Pathology

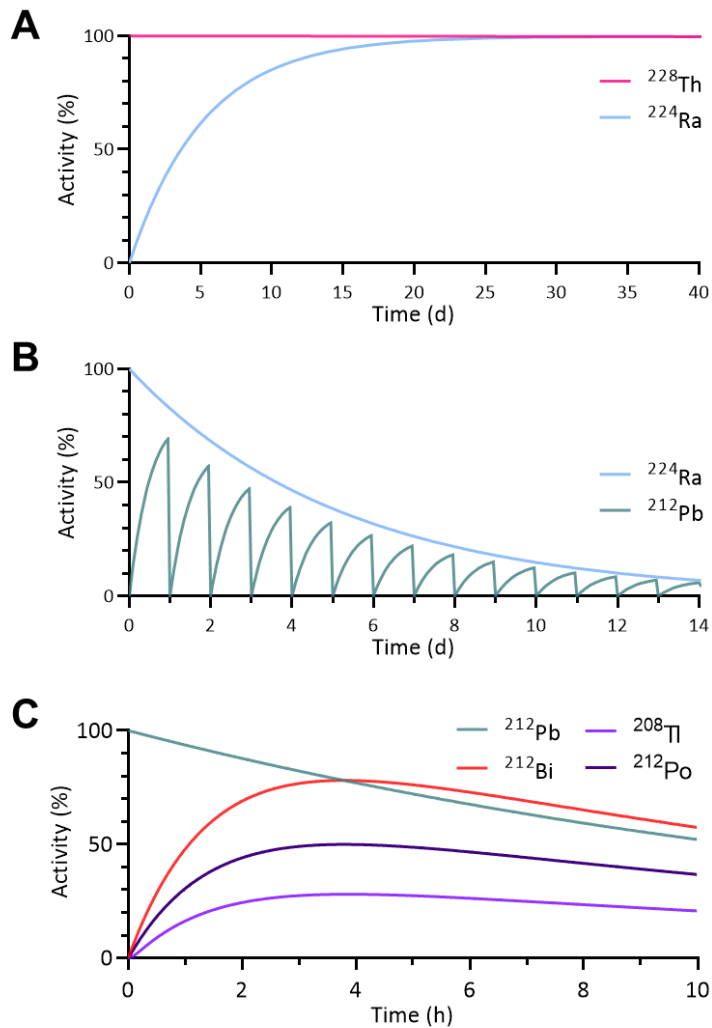
The mice which were submitted alive to LCP ($n = 14$ in total) were comprehensively evaluated by board-certified veterinary pathologists. These mice were euthanized with CO₂, followed by terminal blood collection via cardiac puncture. Following gross examination, all organs were fixed in 10% neutral buffered formalin, followed by decalcification of the bones and other hard tissues in a formic acid solution (Surgipath Decalcifier I, Leica Biosystems). Tissues were processed in ethanol and xylene and embedded in paraffin in a Leica ASP6025 tissue processor. Paraffin blocks were sectioned at 5 microns, stained with hematoxylin and eosin (H&E), and examined by board-certified veterinary pathologists. For all the submitted mice, the following tissues were processed and examined microscopically: xenograft tumor with surrounding tissues, lungs, liver, kidneys, spleen, esophagus, oviducts, bones with bone marrow (vertebrae, sternum, femur, tibia), stifle joint, skeletal muscles, nerves, spinal cord, mammary glands and, when present on the evaluated slides, the gallbladder, ovaries, and lymphoid tissues (cranial deep cervical, superficial parotid, submandibular, axillary, tracheobronchial, mesenteric, renal, inguinal, popliteal lymph node(s), and/or thymus). For three of the submitted mice from the high-dose treated cohort, the following tissues were also processed and examined microscopically: heart, pancreas, stomach, duodenum, jejunum, ileum, cecum, colon, salivary, lacrimal, and harderian glands, skin (perineal, trunk and head), urinary bladder, uterus, cervix, vagina, adrenal glands, thyroid gland, trachea, skull with bone marrow, nasal and oral cavities, teeth, ears, eyes, pituitary gland, and brain.

Hematology and serum chemistry were performed on the blood samples collected via cardiac puncture for the selected treated mice.

For hematology, a portion of the collected blood was transferred into tubes containing EDTA. Automated analysis was performed on an IDEXX Procyte DX hematology analyzer, and the following parameters were determined: white blood cell count, red blood cell count, hemoglobin concentration, hematocrit, mean corpuscular volume, mean corpuscular hemoglobin, mean corpuscular hemoglobin concentration, red blood cell distribution width standard deviation and coefficient of variance, reticulocyte relative and absolute counts, platelet count, platelet distribution width, mean platelet volume, and relative and absolute counts of neutrophils, lymphocytes, monocytes, eosinophils, and basophils.

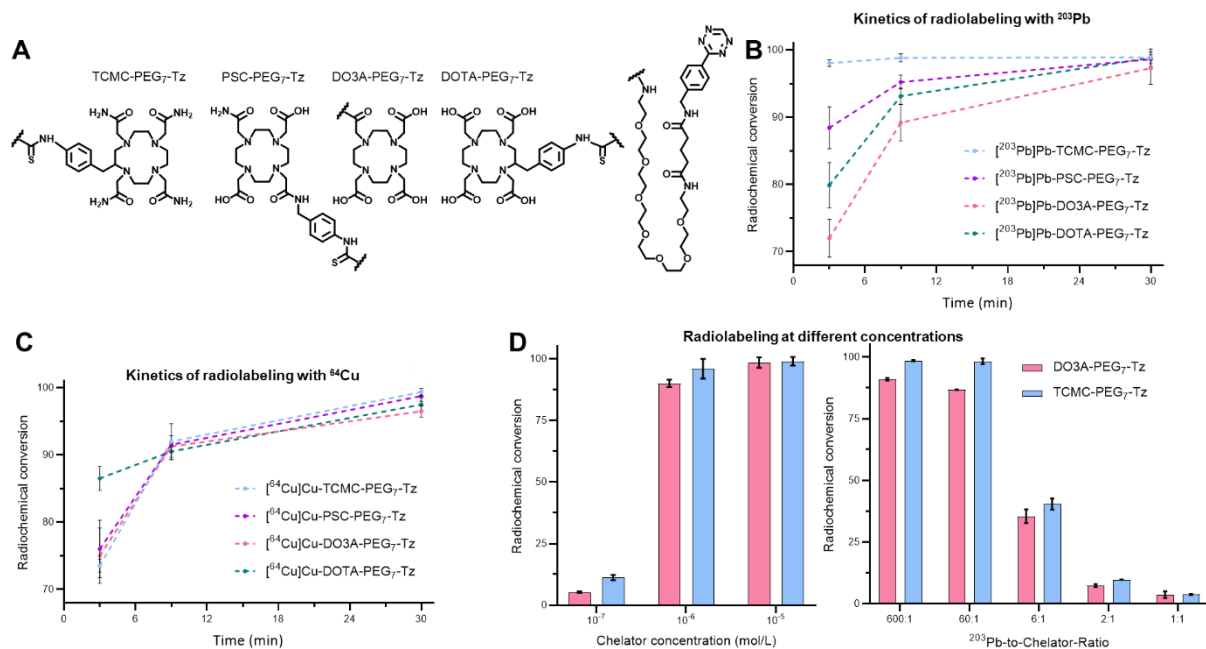
For serum chemistry, a portion of the collected blood was transferred into tubes containing a serum separator, the tubes were centrifuged, and the serum was obtained for analysis. Serum chemistry was performed on a Beckman Coulter AU680 analyzer, and the concentration of the following analytes was determined: alkaline phosphatase, alanine aminotransferase, aspartate aminotransferase, creatine kinase, gamma-glutamyl transpeptidase, albumin, total protein, globulin, direct, indirect and total bilirubin, blood urea nitrogen, creatinine, cholesterol, triglycerides, glucose, total carbon dioxide, calcium, phosphorus, chloride, potassium, and sodium. Na/K, albumin/globulin, blood urea nitrogen/creatinine ratios, and the anion gap were calculated.

2 Figures and tables



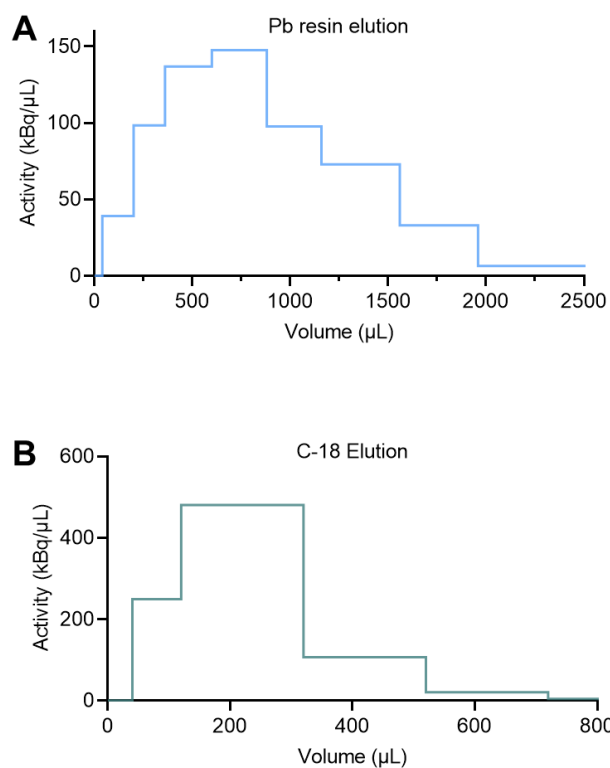
Supplemental Figure 1 ^{228}Th -generator and practical considerations.

A) The graph shows the secular equilibrium between ^{228}Th and ^{224}Ra . The equilibrium is reached after approximately 25 d. **B)** The graph shows the transient equilibrium between ^{224}Ra and ^{212}Pb when performing daily elutions of the $^{224}\text{Ra}/^{212}\text{Pb}$ generator. **C)** The graph shows the equilibrium of ^{212}Ra and its daughters, which is approximately reached 8 h after the purification. The graphs were plotted using the Bateman equation.



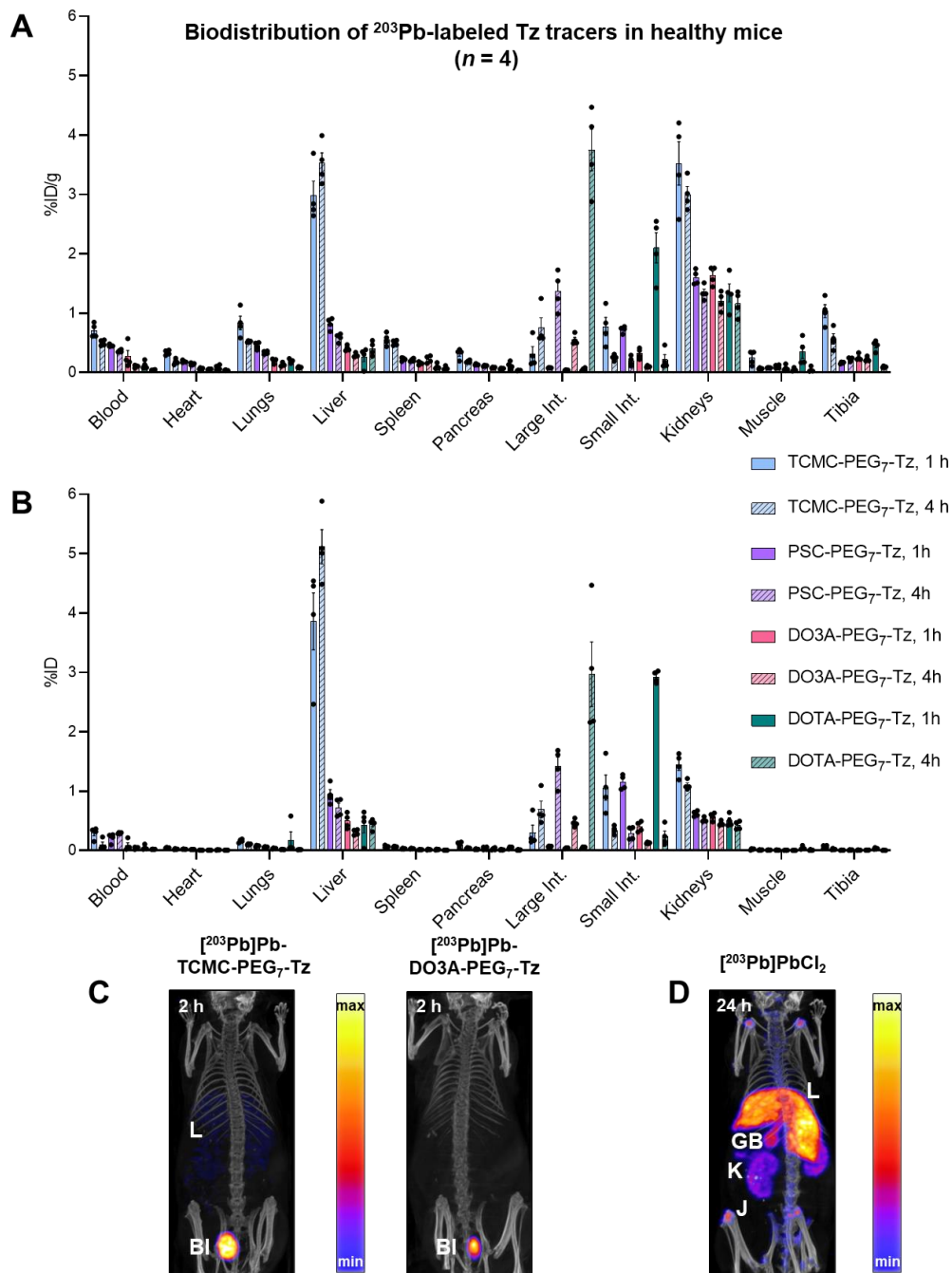
Supplemental Figure 2 Chemical evaluation of the Tz compounds.

A) Chemical structures of the four Tz precursors. **B)** Radiochemical conversion of the four Tz precursors with ²⁰³Pb at different time points measured via radio iTLC. Radiolabeling was performed at 37 °C at a chelator concentration of 10⁻⁶ mol/L. **C)** Radiochemical conversion of the four Tz precursors with ⁶⁴Cu at different time points measured via radio iTLC. Radiolabeling was performed at 37 °C at a chelator concentration of 10⁻⁶ mol/L. **D)** Radiolabeling of DO3A-PEG₇-Tz and TCMC-PEG₇-Tz with ²⁰³Pb. Left: For each labeling, 3.7 MBq of ²⁰³Pb was used and the chelator concentration was varied from 10⁻⁷ to 10⁻⁵ mol/L. Right: The chelator concentration was 10⁻⁶ mol/L and the added activity of ²⁰³Pb was varied from 0.22 GBq to 0.37 MBq.



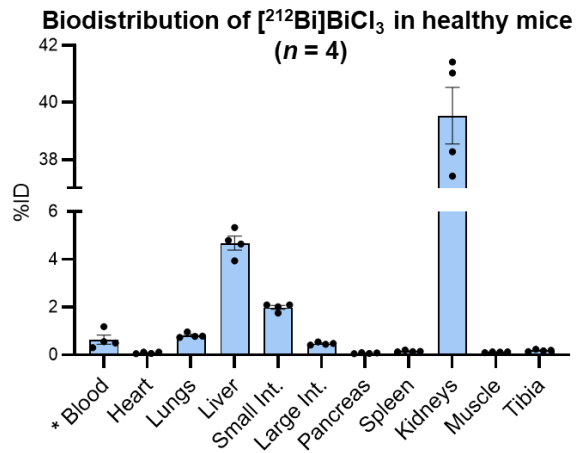
Supplemental Figure 3 Purification of radiolead and the radiotracers.

A) Representation of a typical Pb cartridge elution profile with NH_4OAc (1 M, pH 4.5) from a column containing Pb resin. **B)** Representation of a typical elution profile of a Tz-based radiotracer with ethanol (95 %) from a C-18 cartridge.



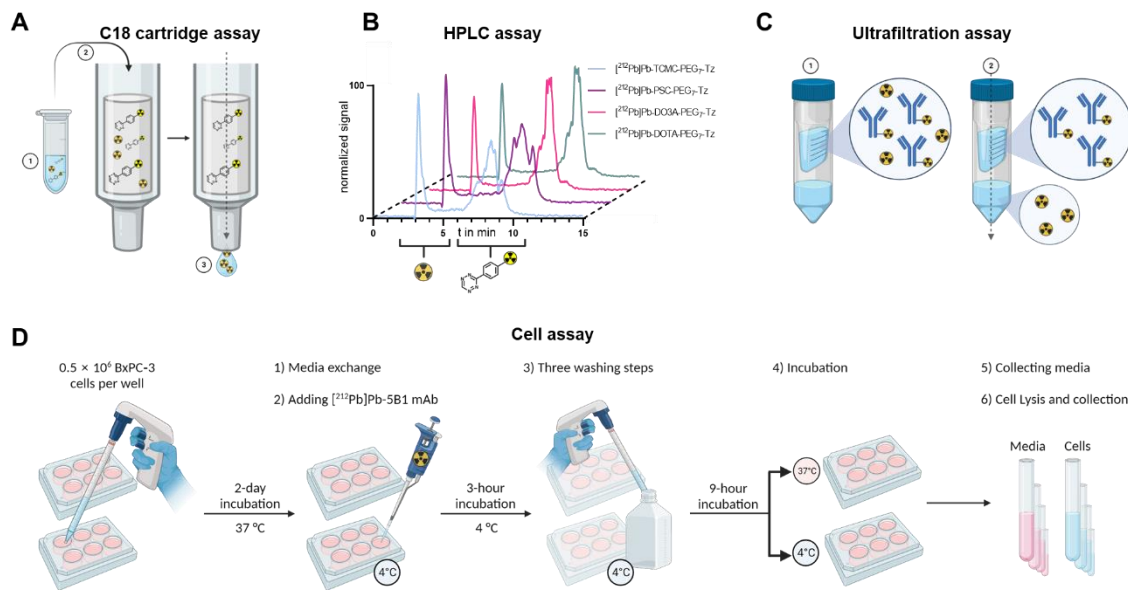
Supplemental Figure 4 Pharmacokinetics of ^{203}Pb -labeled Tz tracers in healthy mice.

Biodistribution data of the four ^{203}Pb -labeled Tz tracers (2 nmol, 0.7 MBq per mouse) at 1 and 4 h post-administration in healthy female nude mice ($n = 4$). Int. = intestines **A**) Representation in percent injected dose per gram of tissue. **B**) Representation in percent injected dose. **C**) SPECT imaging of one healthy female nude mouse, 2 h after receiving 18.5 MBq of ^{203}Pb -TCMC-PEG₇-Tz (left) or ^{203}Pb -DO3A-PEG₇-Tz (right). Uptake can be seen in the liver (L) and bladder (BL). **D**) SPECT imaging of one healthy female nude mouse, 24 h after receiving 18.5 MBq of ^{203}Pb Cl₂. Uptake of unchelated ^{203}Pb can be seen in the joints (J), liver (L), kidneys (K), and gallbladder (GL).



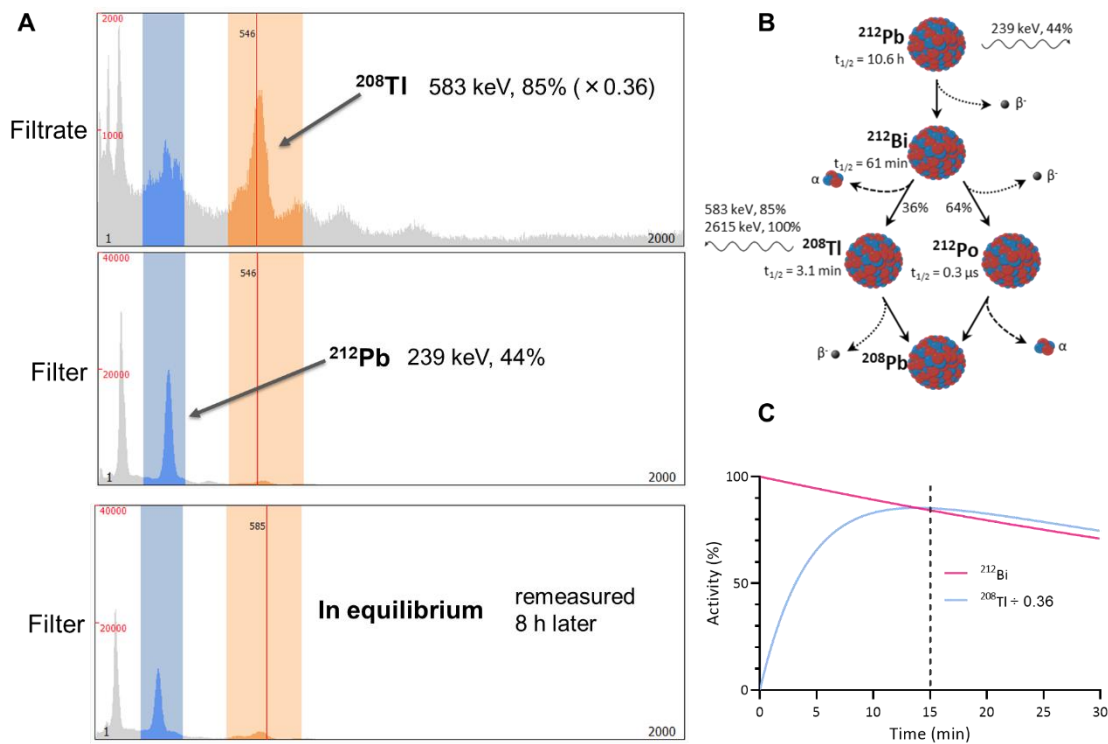
Supplemental Figure 5 Biodistribution data of $[^{212}\text{Bi}]\text{BiCl}_3$.

Biodistribution data of $[^{212}\text{Bi}]\text{BiCl}_3$ (1.9 MBq per mouse) in healthy athymic female nude mice ($n = 4$) at 1 h post injection. The data is represented in percent injected dose. *The activity in the blood pool is corrected for a volume of 2.5 mL (estimated blood volume of a mouse). Int. = intestines.



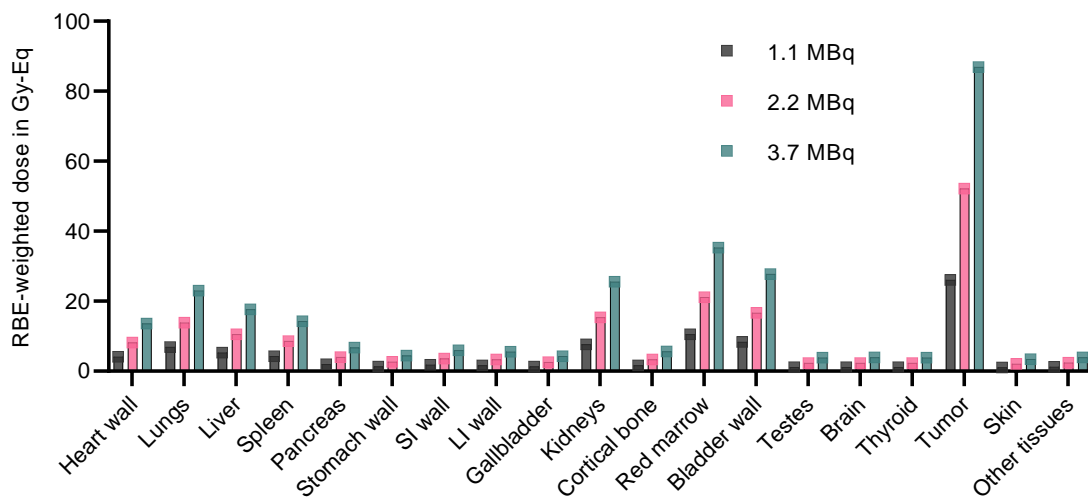
Supplemental Figure 6 Study designs of the *in vitro* ^{212}Bi -release.

A) Scheme of the *in vitro* ^{212}Bi -release study of the ^{212}Pb -labeld Tz tracers via the C18 cartridge assay. **B)** Scheme of the *in vitro* ^{212}Bi -release study of the ^{212}Pb -labeld Tz tracers via the HPLC assay. **C)** Scheme of the *in vitro* ^{212}Bi -release study of ^{212}Pb -labeld mAb conjugates via the ultrafiltration assay. **D)** Study design of the ^{212}Bi -release study in BxPC-3 cells. This figure was partially created with BioRender.



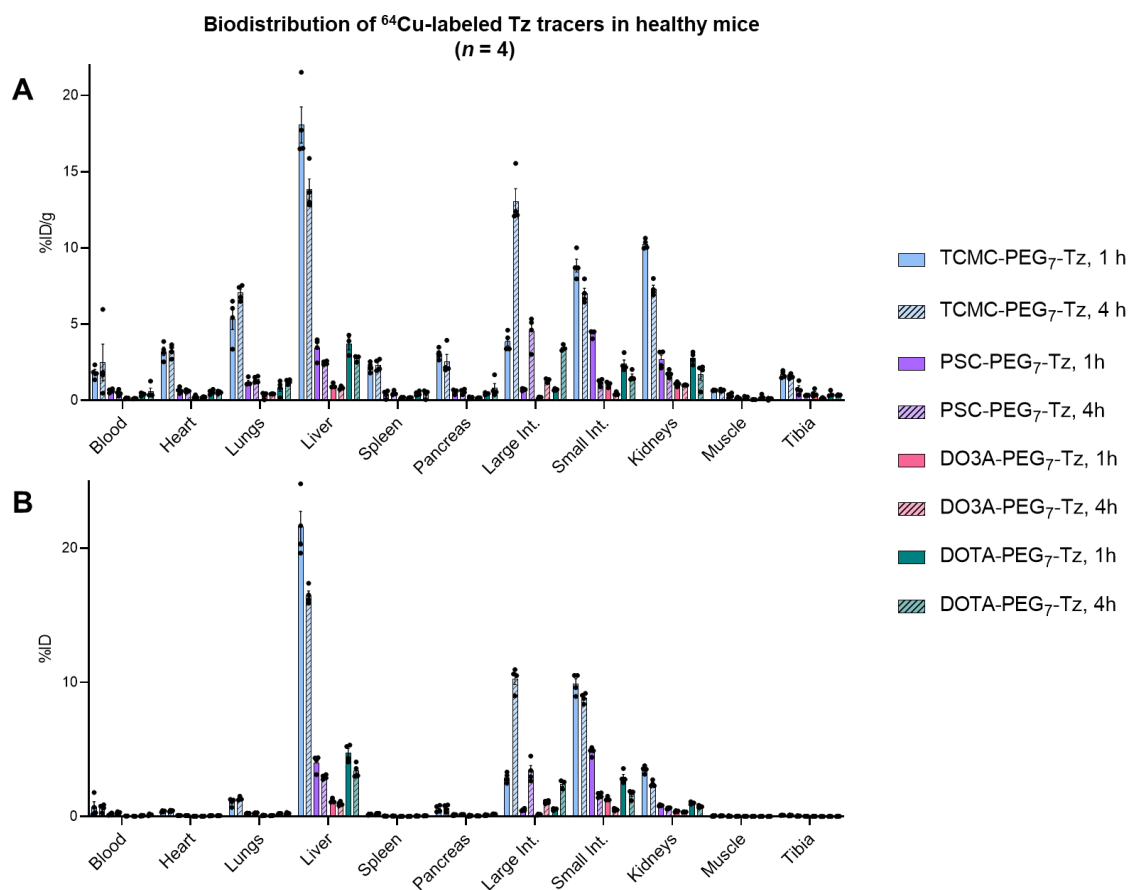
Supplemental Figure 7 Gamma-spectroscopy with ^{212}Pb and ^{208}Tl .

A) Representation of a typical gamma-spectra with window settings for ^{212}Pb and ^{208}Tl of a fraction containing released ^{212}Bi (filtrate) and chelated ^{212}Pb and ^{212}Bi (filter), as obtained in the C-18 cartridge assay. **B)** Lead-212 decay scheme. **C)** The graph (plotted using the Bateman equation) shows the equilibrium between ^{212}Bi and ^{208}Tl . An ideal representation with the gamma-emitting daughter ^{208}Tl of ^{212}Bi is reached after 15 min.



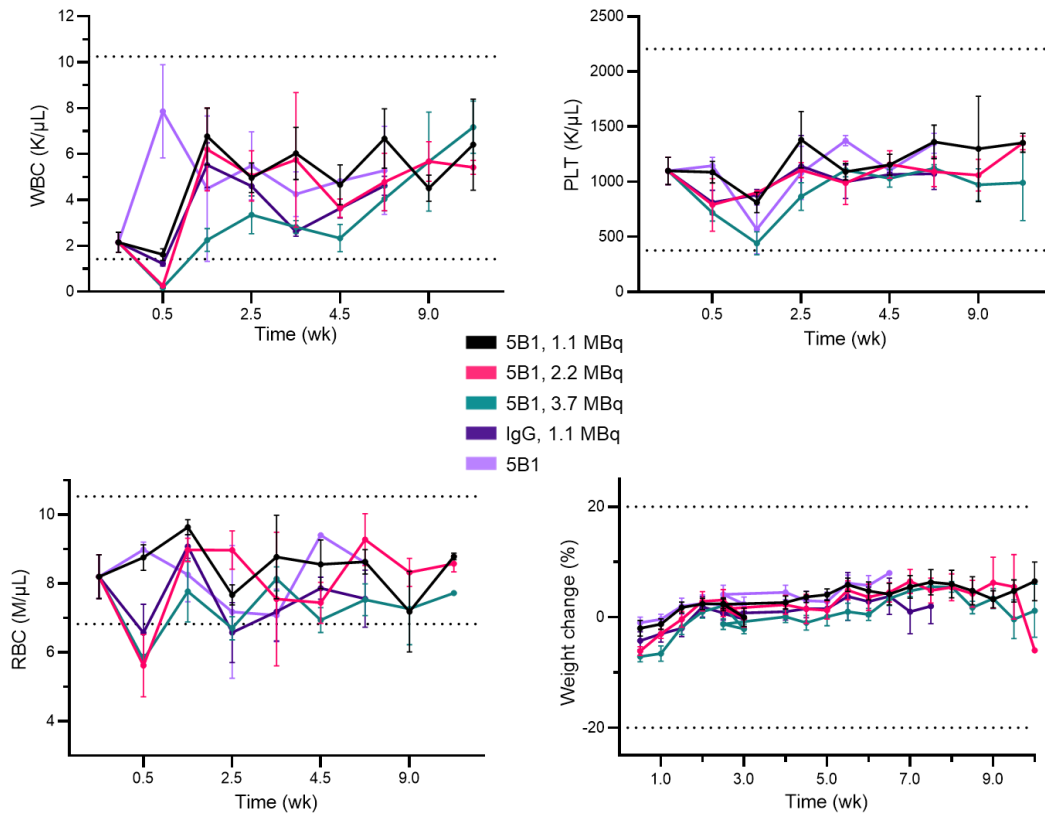
Supplemental Figure 8 RBE-weighted absorbed doses estimated for $[^{212}\text{Pb}]\text{Pb-DO3A-PEG}_7\text{-Tz}$

Relative biological effectiveness-weighted absorbed doses estimated for the administered activities of $[^{212}\text{Pb}]\text{Pb-DO3A-PEG}_7\text{-Tz}$ used in the therapy studies (assuming no redistribution). SI = small intestines, LI = large intestines.



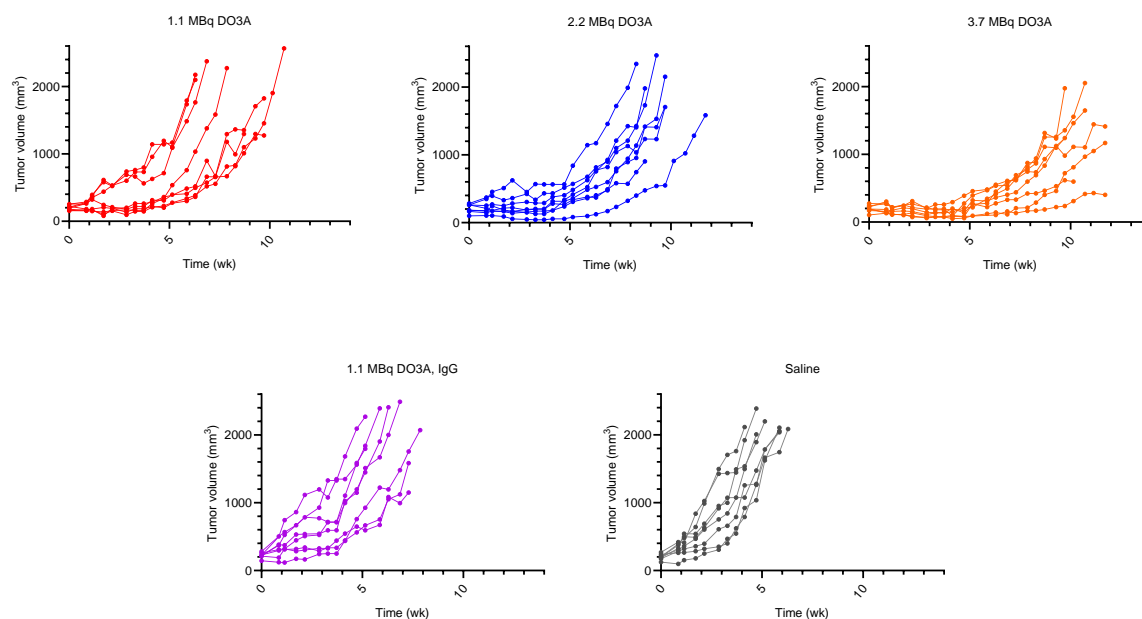
Supplemental Figure 9 Biodistribution data of ^{64}Cu -labeled Tz tracers in healthy mice.

Biodistribution data of the four ^{64}Cu -labeled Tz tracers (2 nmol, 0.7 MBq per mouse) at 1 and 4 h post-administration in healthy female nude mice ($n = 4$). Int. = intestines **A**) Representation in percent injected dose per gram of tissue. **B**) Representation in percent injected dose.



Supplemental Figure 10 Hematological parameters and weights.

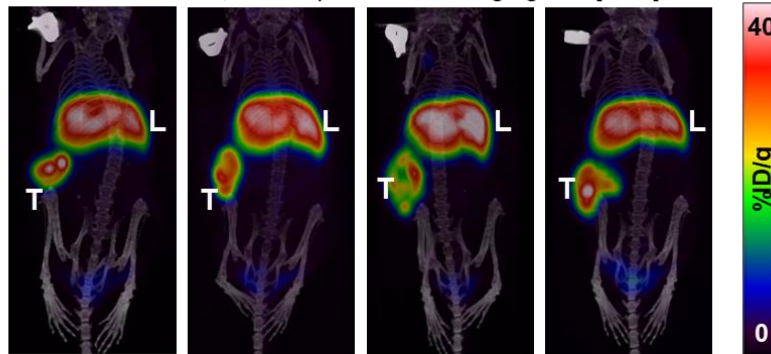
Hematological parameters and relative body weight change during therapy. Complete blood counts analysis was performed weekly on selected mice ($n = 3$ per cohort). On the top: white blood cell counts (WBC) and platelets (PLT). On the bottom: red blood cell counts (RBC), and relative body weight change.



Supplemental Figure 11 Individual tumor growth plots for all cohorts of the therapy study.

The first three graphs present the individual tumor growth of the pretargeted therapy cohorts, which received 1.1, 2.2, 3.7 MBq of $[^{212}\text{Pb}]\text{Pb-DO3A-PEG}_7\text{-Tz}$. The two graphs on the bottom present the individual tumor growth of the control cohorts, which received an unspecific IgG-TCO mAb followed by 1.1 MBq of $[^{212}\text{Pb}]\text{Pb-DO3A-PEG}_7\text{-Tz}$ 3 d later (left), and the cohort which only received 5B1-TCO (right).

4 Mice of the 5B1, 3.7MBq cohort – re-imaging with ^{64}Cu]Cu-5B1



Supplemental Figure 12 Re-imaging with ^{64}Cu]Cu-5B1.

In the tenth week, four mice from the 3.7 MBq group were randomly selected for re-imaging with ^{64}Cu -labeled 5B1 mAb (preconjugated ^{64}Cu]Cu-DO3A-PEG₇-Tz to 5B1-TCO) to confirm that their tumors still highly express the CA 19-9 antigen. Uptake can be seen in tumor (T) and liver (L). The positive tumor uptake highlights that multiple injections of ^{212}Pb]Pb-DO3A-PEG₇-Tz in 1–2 wk intervals would be possible.

Supplemental Table 1 Chemical evaluation of the tetrazine compounds.

Compound	t _R on HPLC (min)	t _R as ^{nat} Pb-chelate on HPLC (min)	log D _{7,4} values (n = 4)
TCMC-PEG ₇ -Tz	8.6	9.7	-2.5 ± 0.1
PSC-PEG ₇ -Tz	8.8	9.2	-2.3 ± 0.1
DO3A-PEG ₇ -Tz	8.4	8.9	-2.0 ± 0.1
DOTA-PEG ₇ -Tz	9.0	9.5	-1.9 ± 0.1

Supplemental Table 2 In vitro bismuth release from the tetrazine compounds.

Compound	C18 cartridge assay (n = 4)	HPLC assay (n = 4)	UF assay (n = 4)
TCMC-PEG ₇ -Tz	(42 ± 5)%	(39 ± 5)%	(44 ± 5)%
PSC-PEG ₇ -Tz	(41 ± 5)%	(40 ± 5)%	(44 ± 5)%
DO3A-PEG ₇ -Tz	(41 ± 5)%	(37 ± 5)%	(46 ± 5)%
DOTA-PEG ₇ -Tz	(43 ± 5)%	(37 ± 5)%	(43 ± 5)%

Supplemental Table 3 RBE-weighted dose calculations assuming in situ decay of the progeny.

	RBE-weighted dose coefficient (Gy/MBq)	RBE-weighted dose (Gy) for 1.1 MBq administration	RBE-weighted dose (Gy) for 2.2 MBq administration	RBE-weighted dose (Gy) for 3.7 MBq administration	Therapeutic index
Heart wall	3.6874	4.0930	8.1860	13.6433	6.3681
Lungs	6.2258	6.9106	13.8212	23.0353	3.7717
Liver	4.7673	5.2917	10.5835	17.6391	4.9255
Spleen	3.8667	4.2921	8.5842	14.3070	6.0727
Pancreas	1.8214	2.0217	4.0434	6.7390	12.8924
Stomach wall	1.2081	1.3410	2.6820	4.4700	19.4368
SI wall	1.6180	1.7960	3.5919	5.9865	14.5130
LI wall	1.5048	1.6704	3.3407	5.5678	15.6043
Gallbladder	1.1517	1.2784	2.5569	4.2615	20.3878
Kidneys	6.9165	7.6773	15.3545	25.5909	3.3950
Cortical bone	1.5159	1.6827	3.3654	5.6089	15.4900
Red marrow	9.5355	10.5844	21.1688	35.2814	2.4626
Bladder wall	7.5022	8.3275	16.6550	27.7583	3.1300
Testes	1.0503	1.1659	2.3317	3.8862	22.3564
Brain	1.0629	1.1798	2.3597	3.9328	22.0917
Thyroid	1.0434	1.1582	2.3165	3.8608	22.5040
Tumor	23.4817	26.0646	52.1293	86.8822	--
Skin	0.9260	1.0279	2.0557	3.4262	25.3583
Other tissues	1.0691	1.1867	2.3733	3.9555	21.9648

Supplemental Table 4 RBE-weighted dose calculations considering the redistribution of the progeny.

	RBE-weighted dose coefficient (Gy/MBq)	RBE-weighted dose (Gy) for 1.1 MBq administration	RBE-weighted dose (Gy) for 2.2 MBq administration	RBE-weighted dose (Gy) for 3.7 MBq administration	Therapeutic index
Heart wall	2.2202	2.4645	4.9289	8.2149	6.3504
Lungs	3.7207	4.1300	8.2599	13.7665	3.7895
Liver	2.8781	3.1947	6.3895	10.6491	4.8988
Spleen	2.3723	2.6333	5.2665	8.7776	5.9434
Pancreas	1.1445	1.2704	2.5409	4.2348	12.3190
Stomach wall	0.7516	0.8343	1.6686	2.7811	18.7583
SI wall	0.9818	1.0898	2.1797	3.6328	14.3604
LI wall	0.9275	1.0295	2.0590	3.4316	15.2022
Gallbladder	0.6424	0.7130	1.4260	2.3767	21.9498
Kidneys	62.3174	69.1723	138.3447	230.5745	0.2263
Cortical bone	0.9128	1.0132	2.0264	3.3774	15.4465
Red marrow	5.7573	6.3906	12.7813	21.3021	2.4490
Bladder wall	4.5942	5.0995	10.1991	16.9984	3.0690
Testes	0.6340	0.7037	1.4075	2.3458	22.2392
Brain	0.6386	0.7088	1.4177	2.3628	22.0793
Thyroid	0.6098	0.6769	1.3539	2.2564	23.1199
Tumor	14.0995	15.6505	31.3009	52.1682	--
Skin	0.5526	0.6134	1.2267	2.0446	25.5154
Other tissues	0.6596	0.7321	1.4643	2.4405	21.3764

References

1. Houghton JL, Zeglis BM, Abdel-Atti D, Sawada R, Scholz WW, Lewis JS. Pretargeted Immuno-PET of Pancreatic Cancer: Overcoming Circulating Antigen and Internalized Antibody to Reduce Radiation Doses. *J Nucl Med.* 2016;57:453-459.
2. Sarrett SM, Keinanen O, Dayts EJ, Dewaele-Le Roi G, Rodriguez C, Carnazza KE, Zeglis BM. Inverse electron demand Diels-Alder click chemistry for pretargeted PET imaging and radioimmunotherapy. *Nat Protoc.* 2021;16:3348-3381.
3. Kozminski P, Gaweda W, Rzewuska M, et al. Physicochemical and Biological Study of ^{99m}Tc and ^{68}Ga Radiolabelled Ciprofloxacin and Evaluation of [^{99m}Tc]Tc-CIP as Potential Diagnostic Radiopharmaceutical for Diabetic Foot Syndrome Imaging. *Tomography.* 2021;7:829-842.
4. Imberti C, Chen YL, Foley CA, et al. Tuning the properties of tris(hydroxypyridinone) ligands: efficient ^{68}Ga chelators for PET imaging. *Dalton Trans.* 2019;48:4299-4313.
5. Mirzadeh S, Kumar K, Gansow OA. The Chemical Fate of ^{212}Bi -DOTA Formed by β -Decay of $^{212}\text{Pb}(\text{DOTA})^{2-}$. *Radiochimica Acta.* 1993;60:1-10.
6. Keenan MA, Stabin MG, Segars WP, Fernald MJ. RADAR realistic animal model series for dose assessment. *J Nucl Med.* 2010;51:471-476.
7. Carter LM, Crawford TM, Sato T, et al. PARaDIM: A PHITS-Based Monte Carlo Tool for Internal Dosimetry with Tetrahedral Mesh Computational Phantoms. *J Nucl Med.* 2019;60:1802-1811.
8. Bartlett RM, Bolch WE, Brill AB, et al. *MIRD Primer 2022: A Complete Guide to Radiopharmaceutical Dosimetry*. SNMMI; 2022.
9. Cloutier RJ, Smith SA, Watson EE, Snyder WS, Warner GG. Dose to the fetus from radionuclides in the bladder. *Health Phys.* 1973;25:147-161.